

Article

Super-resolution single-molecule reconstruction of composite infrared images based on deep machine learning

Jing Xiao^{1,2}, Yubo Zhang³, Chong Liu¹, Haimei Liu¹, Yalei Dong^{1,*}¹ Hebei Chemical and Pharmaceutical College, Shijiazhuang 050026, China² School of Electrical and Information Engineering, Tianjin University, Tianjin 300072, China³ Institute of Software, Chinese Academy of Sciences, Beijing 100190, China* **Corresponding author:** Yalei Dong, dylxoxiang@163.com

CITATION

Xiao J, Zhang Y, Liu C, et al. Super-resolution single-molecule reconstruction of composite infrared images based on deep machine learning. *Molecular & Cellular Biomechanics*. 2025; 22(2): 1169. <https://doi.org/10.62617/mcb1169>

ARTICLE INFO

Received: 19 December 2024

Accepted: 3 January 2025

Available online: 10 February 2025

COPYRIGHT



Copyright © 2025 by author(s).
Molecular & Cellular Biomechanics
is published by Sin-Chn Scientific
Press Pte. Ltd. This work is licensed
under the Creative Commons
Attribution (CC BY) license.
<https://creativecommons.org/licenses/by/4.0/>

Abstract: In order to improve the resolution of infrared images of single-molecule reconstruction of composite materials, this paper proposes an image super-resolution reconstruction method based on deep machine learning SRGAN. By replacing the residual blocks of the generated network in SRGAN with residual dense block, it can more effectively acquire and utilize the image features from various network layers, especially those containing high-frequency information, thereby ensuring that more details and textures are preserved during the magnification of infrared images. The SE attention mechanism is incorporated into the generative network by assigning a weight to each channel, which strengthens the focus on important features while reducing reliance on irrelevant information. Super-resolution reconstruction experiments conducted on CFRP composite material infrared images demonstrate that the improved algorithm achieves a 0.6 increase in Peak Signal-to-Noise Ratio (PSNR) and a 0.3% increase in Structural Similarity Index (SSIM) compared to SRGAN, providing valuable references for the super-resolution reconstruction of infrared images of composite materials.

Keywords: super resolution reconstruction; infrared image; molecule; composite material; deep learning

1. Introduction

Carbon Fiber Reinforced Polymer (CFRP) has been widely used in many fields [1–5]. However, during the material processing, defects such as cracks and inclusions can easily occur, which affect the material's performance and safety. Timely detection of defects in composite materials is essential for maintaining their exceptional performance and ensuring safety. Given the intricate nature of composite structures, defects can significantly compromise their integrity and functionality. Early identification of these flaws not only safeguards against potential failures but also enhances the longevity and reliability of the materials. In this context, the application of single molecule techniques offers new insights into defect detection, potentially improving accuracy and efficiency in identifying issues [6–8]. Infrared imaging technology is highly effective in identifying concealed defects during the single-molecule reconstruction of composite materials. This advanced technique leverages thermal signatures to reveal inconsistencies that may not be visible through conventional inspection methods. By providing detailed insights into the material's internal structure, infrared imaging enhances the accuracy of defect detection, ensuring the integrity and reliability of composite components in various applications. This capability is particularly crucial in industries where performance and safety are

paramount, such as aerospace and automotive engineering [9–11]. However, the constraints imposed by shooting distance and the complexities of various environments significantly diminish the resolution of infrared images, hindering the precise identification of defects in composite materials [12]. To address these challenges, we leverage advanced deep learning image processing technology to optimize infrared imagery. This approach not only enhances the resolution of the images but also significantly improves the accuracy and efficiency of defect detection in composite materials. By ensuring higher quality and reliability, our method contributes to the overall integrity of the mat.

Harris et al. [13] first proposed the concept of image super-resolution. With the development of the field of deep learning, the super-Resolution Convolutional Neural Networks (SRCNN) proposed by Dong et al. [14] has become a milestone in this field. Ledig et al. [15] proposed the Super-Resolution Generative Adversarial Network (SRGAN), which successfully combined the super-resolution reconstruction technology with the generative adversarial networks, achieving significant breakthroughs in the field of super-resolution reconstruction. Wu et al. [16] proposed an image super-resolution reconstruction algorithm based on lightweight and dense residual networks (I-SRGAN), which achieved good reconstruction results in experiments on ultra-resolution reconstruction of insulator infrared images in transmission lines. Liu et al. [17] proposed an infrared image super-resolution reconstruction algorithm that integrates residual dense and generative adversarial networks, which effectively improves the image quality. Hu et al. [18] proposed an efficient and low-cost super-resolution method for infrared images by combining generative adversarial networks with lightweight attention residual blocks, focusing on the reconstruction of detailed textures and the accurate extraction of pixel features.

2. SRGAN

SRGAN is a cutting-edge image super-resolution technology that harnesses the principles of generative adversarial networks (GANs). This innovative approach involves a dynamic interplay between two neural networks: the generator and the discriminator.

The generator network is tasked with creating high-resolution images from their low-resolution counterparts, effectively enhancing the visual quality and detail. Meanwhile, the discriminator network plays a critical role by assessing the generated high-resolution images against authentic high-resolution images, thereby identifying discrepancies and guiding the generator towards improved accuracy.

This adversarial learning process not only facilitates the transformation of low-resolution images into high-resolution ones but also ensures that the generated outputs are as realistic and detailed as possible. The flowchart illustrating this process is depicted in **Figure 1**.

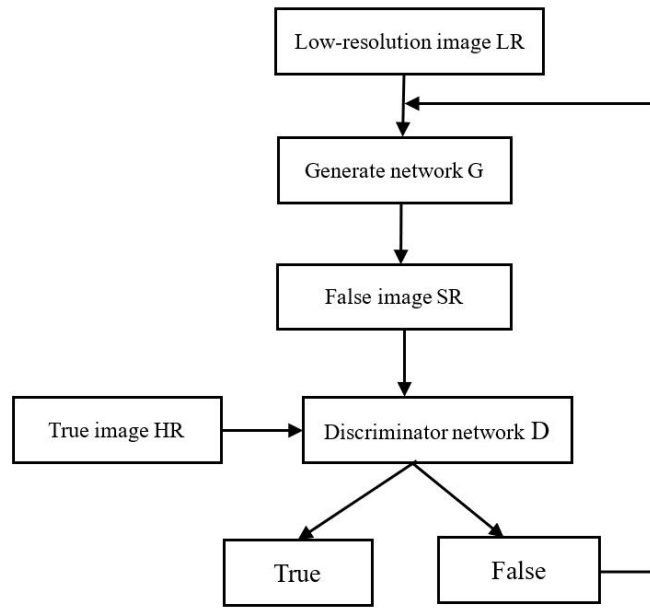


Figure 1. SRGAN flowchart.

2.1. SRGAN network structure

The network structure of SRGAN (Super-Resolution Generative Adversarial Network) mainly consists of two parts: the generator network and the discriminator network, as shown in Figures 2 and 3.

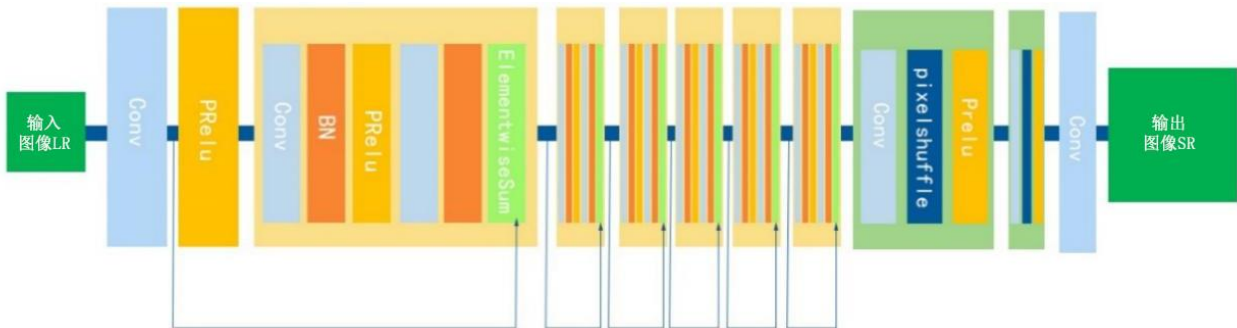


Figure 2. Generator network structure.



Figure 3. Discriminant network structure.

The generator network is comprised of several residual blocks, which effectively mitigate issues related to gradient vanishing and training bottlenecks. In the final layers of the generator, upsampling is performed through subpixel convolution. This method is a highly efficient technique for upsampling, as it enhances the image resolution by reorganizing the spatial dimensions of the feature map.

The discriminator network is composed of multiple convolutional layers, each utilizing filters to convolve the input image and produce a corresponding feature map. Following these convolutional layers, one or more fully connected layers are typically employed to map the extracted features to the output space. The output space is usually a single dimension, which represents the probability that the input image is an authentic, real image. This architecture enables the discriminator to effectively distinguish between real and generated images, thereby enhancing the overall performance of the generative adversarial network.

2.2. Loss function

The loss function is mainly used to measure the degree of error between the model's prediction results and the true results. Generally, the smaller the loss function, the better the prediction performance of the model. The loss function of SRGAN is important for generating the network, which includes both content loss and adversarial loss. The loss function formula of SRGAN is shown in Equation (1), which $l_{Content}^{SR}$ is the content loss, l_{Gen}^{SR} is the confrontation loss. The loss function of SRGAN weights both the content loss and the confrontation loss by certain weights to balance the role of both in the training process. This design allows SRGAN to generate more realistic and rich super-resolution images while maintaining the similarity of the image content.

$$l^{SR} = l_{Content}^{SR} + 10^{-3}l_{Gen}^{SR} \quad (1)$$

3. Improved SRGAN model

SRGAN has the following shortcomings in infrared image reconstruction of composite materials:

- 1) Due to the low resolution of the infrared image themselves, as well as the impact of infrared imaging devices and the environment, infrared images usually present low contrast, unclear target edges and other shortcomings. SRGAN algorithm may not be able to completely overcome these problems in the reconstruction process, resulting in the resolution of the reconstructed image is not high enough to meet the needs of some applications;
- 2) SRGAN distributes the weights equally when processing the feature information, and the useless and useful feature information in the reconstructed infrared image is amplified equally, resulting in the reconstructed infrared image containing too much noise and interference information, which affects the detection and recognition performance of the later image.
- 3) The shallow depth of SRGAN network structure limits its ability to extract complex feature information; In view of the above problems, we improve and optimize it.

3.1. The residual module is replaced with the residual dense module

The generation network of SRGAN comprises six residual blocks, which are crucial for image super-resolution algorithms as they aim to recover as much lost detail as possible when scaling small images to high resolution. To enhance this detail recovery further, the original residual network has been replaced with a residual dense

network. This modification leverages the capability of the residual dense network to more effectively capture and utilize image features across various network layers, particularly those rich in high-frequency information. As a result, this approach ensures that more details and textures are preserved during the image amplification process. Additionally, the integration of single molecule analysis techniques could provide deeper insights into the structural nuances of images, potentially improving the overall quality of the super-resolved outputs.

Residual dense network [19] is a deep convolutional neural network structure with significant influence in the field of computer vision and deep learning. It combines the concepts of residual connection and dense connection, and aims to solve the problems such as gradient disappearance and feature sparsity during the traditional neural network training process, thus improving the model performance and convergence speed. In image super-resolution tasks, residual dense networks can learn richer image details and improve the quality and detail recovery ability of low-resolution images. The structure of the residual-dense network is shown in **Figure 4**.

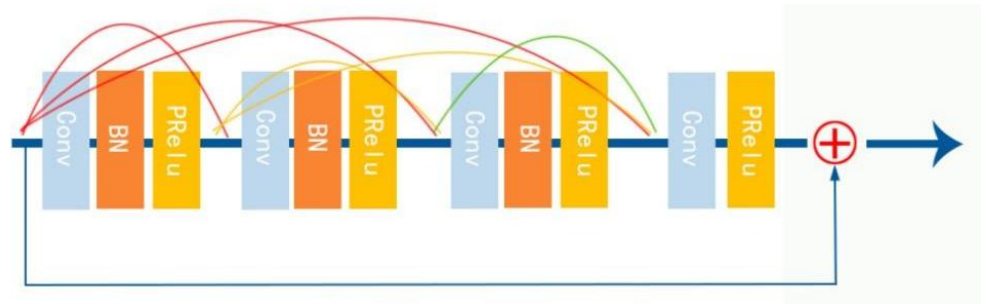


Figure 4. The residual dense network.

The improved generator network structure is shown in **Figure 5**. Through experimental verification, this method not only visually improves the quality of the image, but also significantly surpasses the traditional SRGAN method in objective evaluation indicators, proving the effectiveness and practicability of the improvement in improving the image quality.

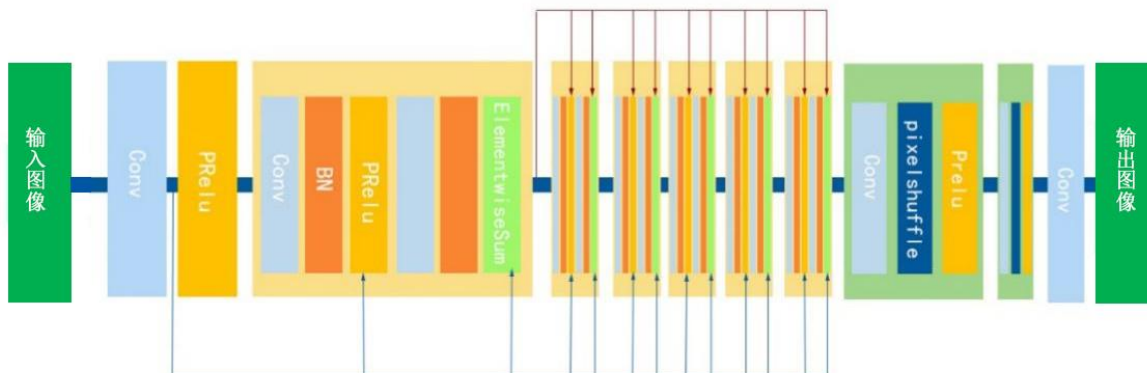


Figure 5. The improved generative network.

3.2. SENet attention mechanism

When humans see an image, they first quickly scan the global image, and then focus on the area of interest. The design of the attention mechanism is inspired by the simulation of the human visual attention mechanism, which not only improves the network's attention to important features, but also enhances the robustness of the network to noise and redundant information, thereby improving the performance of the model. Due to the single color and channel of infrared images of composite materials, the SENet attention mechanism is considered in this paper.

The idea of SENet is very intuitive and effective. By introducing an attention mechanism at the level of the feature channel and assigning a weight to each channel, it enhances the attention to important features while reducing the dependence on useless information. The implementation of this mechanism is relatively simple, but it can significantly improve the model performance. It is widely welcomed and applied because of its ease to integrate into various existing convolutional neural network structures and can bring significant performance improvements without introducing excessive computational complexity. The working principle of SENet is shown in **Figure 6**.

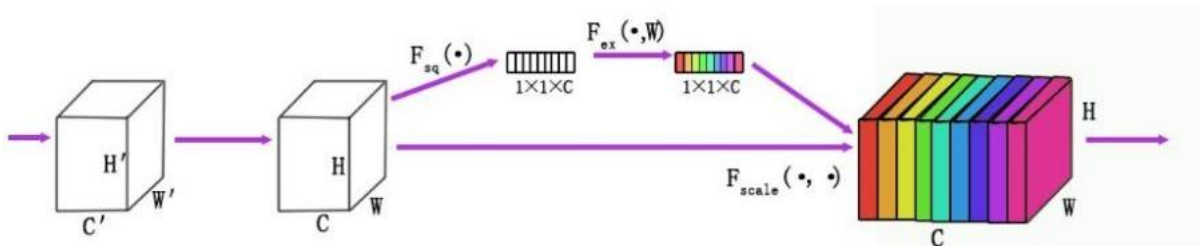


Figure 6. SENet working schematic.

The implementation of SENet is mainly summarized in three steps. The first is Squeeze. Global Average Pooling (GAP) is performed on the input feature map ($H \times W \times C$) to output the feature map of $1 \times 1 \times C$. The next step is to Excitation the feature map. where the compressed feature map is fed into a ReLU activation function, producing a vector of middle_channels. This vector then passes through a fully connected layer and a Sigmoid activation function, yielding a vector with the same number of channels as the input, where each value represents the weight for the corresponding channel. Finally, the channel weights obtained in the previous step are multiplied with the original feature map to obtain the feature map weighted by the attention mechanism. After the convolutional layer of SRGAN, an SE module can be added to assign weights to each feature channel and optimize the extracted content, thus improving the accuracy of the discriminant network.

3.3. Remove the BN layer

The introduction of batch normalization layer into the whole network usually helps to accelerate the training and convergence process, reduce the risk of gradient disappearance, and prevent overfitting to some extent. These advantages are fully verified in tasks such as image classification. However, the application of the BN layer in the image super-resolution task brings different challenges. Specifically, the BN layer tends to reduce absolute differences between data samples while highlighting

relative differences, which partly limits the ability of the model to generalize when dealing with training and test sets with large differences. Therefore, although the BN layer performs well in tasks such as image classification, its effect is not ideal in image super-resolution tasks.

Rise to the challenge, we remove BN layers in the generative network. The BN layer needs to calculate the mean and the variance during the training process, and perform the normalization operation, and these steps all require additional computational resources. However, in the absence of the BN layer, the network can more directly learn the mapping relationship between input and output, and thus can more efficiently handle image super-resolution tasks.

Therefore, in the image super-resolution task, removing the BN layer can not only improve the generalization ability and robustness of the model, but also help to reduce the computational cost and improve the overall performance.

4. Experiments

4.1. Environment

This experiment was completed on the Window system, the hardware selection of TUF-RTX4080S-016G-GAMING graphics card, CPU I7-13700 KF, memory 32G \times 2, the experiment using PyTorch framework, Anaconda3, python3.8.

4.2. Datasets

Composite thermal imaging dataset CFRP, examined by pulsed thermal imaging, is 300 mm \times 300 mm \times 2 mm, three carbon fiber reinforced plastics (CFRP) plates and three glass fiber reinforced plastics (GFRP) plates, each containing 25 inserts with a length/depth ratio between 1.7 and 75. Using two FX60 BALCAR photographic flashes (6.2 kJ per flash) generating thermal pulses (2 ms duration), a X6900 FLIR infrared camera using RerechIR software to record thermal images and customize, we first converted the csv format files into infrared images, from which we selected 12,000 experiments, 10,000 for the training set and 2000 for the test set.

4.3. Parameters

In the training process of the model in this paper, BatchSize is set to 32, and the initialized learning rate is $1e-4$, after 100 iterations. Experiments were performed with a super-resolution reconstruction of a multiple of 4. Training was optimized using the Adam algorithm.

4.4. Evaluation

Both objective and subjective evaluation are important image quality evaluation methods in super-resolution reconstruction algorithms. Common and objective evaluation indicators include:

Peak signal-to-noise ratio (PSNR) is a common measure of the level of image distortion or noise level. Higher values indicate better image quality. According to the numerical range of PSNR, we can have a general assessment of the reconstructed image quality: when PSNR has a value greater than 40 dB, this usually means that the

reconstructed image quality is very high. When the value of PSNR was between 30 and 40 dB, this indicated good quality reconstructed images.

Structural similarity index measurement (SSIM) takes into account the similarity of image structure and measures the similarity between two images based on brightness, contrast and structural information. The closer the SSIM value is to 1, the higher the image quality is.

Subjective evaluation depends on the visual perception of the judge. In super-resolution reconstruction, the Mean Opinion Score (MOS) is usually used for subjective evaluation. The MOS is obtained by averaging the scores given by a group of reviewers. The judges rated the reconstructed images based on their visual performance. The higher the MOS value, the better the quality of the reconstructed image is subjectively.

4.5. Results

In this paper, two indexes of peak signal-to-noise ratio (PSNR) and Structural Similarity Index (SSIM) are selected to compare and judge. At the same time, experiments are compared with algorithms such as Bic, SRCNN, ESPCNN, EDSR, SRGAN. The experimental results are shown in **Table 1**.

Table 1. Comparison of experimental results of 4 x image reconstruction by different algorithms.

model	PSNR	SSIM
Bic	28.05	0.78
SRCNN	31.78	0.81
ESPCN	30.53	0.79
EDSR	30.61	0.81
SRGAN	34.36	0.89
Ours	34.96	0.89

As can be seen from the data in **Table 1**, algorithms based on convolutional neural networks, such as SRCNN and EDSR, have shown excellent performance in super-resolution reconstruction. These algorithms optimize the error value between the original high-resolution image and the super-resolution image generated by the generator, so that the PSNR value of the reconstructed image is higher than that of the traditional algorithm. Therefore, from the perspective of objective evaluation, the super-resolution reconstruction algorithm based on convolutional neural network performs better. The algorithm proposed in this paper is significantly superior to other algorithms in the two key indexes of peak signal-to-noise ratio (PSNR) and structural similarity index (SSIM). This means that the algorithm in this paper performs better in the quality of reconstructed images.

Figure 7 shows the infrared images of composite materials reconstructed by different algorithms. Through observation, we can find that the traditional Bic algorithm is fuzzy when processing image edges and fails to fully retain details. SRGAN and EDSR algorithms surpass Bic in image reconstruction effect. In particular, the SRGAN algorithm not only generates images with higher clarity, but

also more closely resembles the original high-resolution images in texture and detail. Finally, the improved algorithm proposed in this paper realizes the further improvement of image quality. As can be seen from the figure, the image reconstructed by the improved SRGAN algorithm not only maintains texture and detail information, but also presents a better overall visual effect.

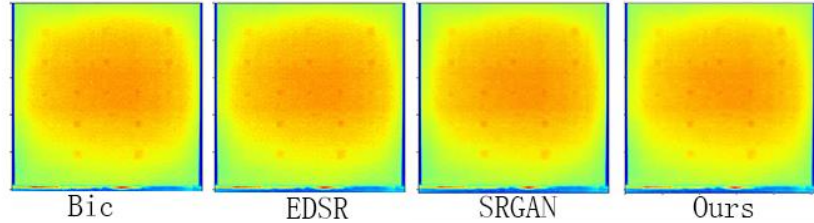


Figure 7. Images reconstructed by the different algorithms.

5. Ablation

In order to verify the enhancement effect of RDN residual-dense network and SENet attention on network training proposed in this paper, ablation experiments are conducted here. Initially, only the generator of the original SRGAN is improved, RDN is replaced by RN network for training; Then, SENet attention mechanism was added into the generation network for training, and the training results are shown in **Table 2**.

Table 2. Comparison of the results of the ablation experiments.

model	PSNR	SSIM
SRGAN	34.363	0.894
SRGAN (residue-dense)	34.913	0.895
SRGAN (Residual-dense + SElayer)	34.967	0.897

As can be seen from **Table 2**, after replacing RN with RDN in SRGAN, PSNR has been significantly improved. Compared with before, PSNR has been increased by 0.55 and SSIM by 0.001. After adding SENet, the increase in PSNR was 0.604 and the increase in SSIM was 0.003.

6. Conclusion

In this paper, we present an enhanced SRGAN method that significantly elevates the quality of infrared image reconstruction. By optimizing the SRGAN framework, we incorporate residual-dense blocks in place of traditional residual blocks. This strategic modification enables the model to extract more comprehensive information across multiple feature layers, resulting in sharper textures and finer details in the reconstructed images.

Additionally, we introduce the Squeeze-and-Excitation (SE) attention mechanism, which further refines the model's ability to focus on relevant features, enhancing its performance. Our approach also integrates deep machine learning techniques, allowing for more sophisticated analysis and processing of image data. Furthermore, the application of single molecule analysis could provide additional insights into the structural nuances of the images.

Experimental validation demonstrates that our improved SRGAN achieves notable advancements in infrared image reconstruction tasks. Specifically, PSNR index shows an improvement of 3.18 over the SRCNN method and 0.6 over the original SRGAN. Similarly, in terms of the Structural Similarity Index (SSIM), our method outperforms others with a gain of 0.08 compared to SRCNN and 0.003 compared to SRGAN.

Beyond these objective quantitative metrics, our method excels in subjective visual assessments. The reconstructed images exhibit superior structural similarity, enhanced edge sharpness, optimal overall brightness, and improved smoothness compared to competing algorithms. This advancement holds significant engineering value for the post-processing of extensive infrared image datasets, particularly in practical applications such as defect detection in composite materials.

In summary, by integrating residual-dense blocks, the SE attention mechanism, and deep machine learning techniques, we have successfully enhanced the SRGAN architecture, leading to a marked improvement in the quality of infrared image reconstruction. This work provides robust technical support for ongoing research and practical applications in related fields.

Author contributions: Conceptualization, JX and YD; methodology, YZ; software, JX; validation, HL; formal analysis, CL; investigation, JX; resources, JX and YD; data curation, YD; writing—original draft preparation, JX and YZ; writing—review and editing, YD; visualization, YZ; supervision, HL; project administration, YD; funding acquisition, JX and YD. All authors have read and agreed to the published version of the manuscript.

Funding: This research was funded by S&T Program of Hebei grant number 236Z2003G, Social Science Development Research Project of Hebei grant number 202403107 and Science Research Project of Hebei Chemical and Pharmaceutical College grant number YS2024018.

Ethical approval: Not applicable.

Conflict of interest: The authors declare no conflict of interest.

References

1. Kupski J, de Freitas ST. Design of adhesively bonded lap joints with laminated CFRP adherends: Review, challenges and new opportunities for aerospace structures[J]. *Composite Structures*, 2021, 268: 113923.
2. Stoiber N, Hammerl M, Kromoser B. Cradle-to-gate life cycle assessment of CFRP reinforcement for concrete structures: Calculation basis and exemplary application[J]. *Journal of Cleaner Production*, 2021, 280: 124300.
3. Mahdavi M, Yousefi E, Baniassadi M, et al. Effective thermal and mechanical properties of short carbon fiber/natural rubber composites as a function of mechanical loading[J]. *Applied Thermal Engineering*, 2017, 117: 8–16.
4. Li D. Carbon fiber reinforced composites make the aircraft structure lighter and stronger [J]. *Large Aircraft*, 2020 (02): 76–79.
5. Zhao Y. Application of advanced fiber-reinforced resin-based composites in the aerospace industry [J]. *Dual-use Technologies and Products*, 2010 (1): 4–6.
6. Jiang H, Chen L. Application of infrared thermal wave imaging in nondestructive detection of composites [J]. *Nondestructive testing*, 2018,40 (11): 37–41.

7. Dou LX, Wang Q, Chen G. Study on the low-speed impact characteristics and damage analysis of carbon fiber composites [J]. *Mechanical and electrical Engineering*, 2016,33 (7): 815–821.
8. Lin L, Fu X, Huang X, et al. Infrared thermal imaging study for the detection of defects in composite materials [J]. *Electromechanical Engineering*, 2019,36 (06): 628–632.
9. Wei X, Xiong J, Wang J, Xu W. Progress in the cellular structure of fiber reinforced composites [J] *Chinese Science: Technical Science*, 2020,50 (08): 1123–1124.
10. Wei J, Liu J, He L, et al. Research and development status of nondestructive testing technology for infrared thermal imaging [J]. *Journal of Harbin University of Science and Technology*, 2020,25 (02): 64–72.
11. An S. Research on infrared thermal wave detection of CFRP laminate [D]. Heilongjiang University of Science and Technology, 2023.
12. Kong S, Xie Y, Wang S, et al. Review of the development of infrared thermal image enhancement algorithm [J]. *Journal of Chongqing University of Science and Technology (Natural Science Edition)*, 2021,23 (04): 77–83.
13. Harris JL. Diffraction and Resolving Power [J]. *Journal of the Optical Society of America*, 1964, 54(7): 931–933.
14. Dong C, Loy C, He K, et al. Image super-resolution using deep convolutional networks[J]. *IEEE transactions on pattern analysis and machine intelligence(S0162–8828)*, 2015, 38(2): 295–307.
15. Ledig C, Theis L, Huszar F, et al. Photo-realistic single image super-resolution using a generative adversarial network[C]// *Proceedings of the IEEE conference on computer vision and pattern recognition*.2017:4681–4690.
16. Wu T, Yang W, Tao X, et al. Super-resolution reconstruction of infrared images of transmission line insulators based on a lightweight, dense residual network [J / OL]. *High-voltage electrical appliances*, 1–12 [2024-06-27].
17. Liu Z, Tao Y, Liu H, et al. Super-resolution reconstruction of infrared patrol images incorporating residual dense and generative adversarial networks [J]. *Journal of Kunming University of Science and Technology (Natural Science edition)*, 2023,48 (05): 120–129.
18. Hu D, Min T. Infrared image super-resolution method for a modified lightweight GAN [J]. *Small Microcomputer system*, 2022,43 (08): 1711–1717.
19. Zhang Y, Tian Y, Kong Y, et al. Residual Dense Network for Image Super-Resolution[C]//*IEEE Conference on Computer Vision & Pattern Recognition*.2018.